Pre-Steady-State Kinetics of RB69 DNA Polymerase and Its Exo Domain Mutants: Effect of pH and Thiophosphoryl Linkages on 3′−5′ Exonuclease Activity†

C. X. Wang, E. Zakharova, J. Li, C. M. Joyce, J. Wang, and W. Konigsberg*

Department of Molecular Biophysics and Biochemistry, Yale University, 333 Cedar Street, New Haven, Connecticut 06520

Received October 29, 2003

ABSTRACT: DNA polymerases from the A and B families with 3′−5′ exonucleolytic activity have exonuclease domains with similar three-dimensional structures that require two divalent metal ions for catalysis. B family DNA polymerases that are part of a replicase generally have a more potent 3′−5′ exonuclease (exo) activity than A family DNA polymerases that mainly function in DNA repair. To investigate the basis for these differences, we determined pH−activity profiles for the exonuclease reactions of T4, RB69, and ϕ29 DNA polymerases as representatives of B family replicative DNA polymerases and the Klenow fragment (KF) as an example of a repair DNA polymerase in the A family. We performed exo assays under single-turnover conditions and found that excision rates exhibited by the B family DNA polymerases were essentially independent of pH between pH 6.5 and 8.5, whereas the exo activity of KF increased 10-fold for each unit increase in pH. Three exo domain mutants of RB69 polymerase had much lower exo activities than the wild-type enzyme and exhibited pH−activity profiles similar to that of KF. On the basis of pH versus activity data and elemental effects obtained using short double-stranded DNA substrates terminating in phosphorothioate linkages, we suggest that the rate of the chemical step is reduced to the point where it becomes limiting with RB69 pol mutants K302A, Y323F, and E116A, in contrast to the wild-type enzyme where chemistry is faster than the rate-determining step that precedes it.

DNA polymerases represent the major component of the replisome, a multicomponent biological machine responsible for faithfully replicating cellular and viral DNA. In addition to the nucleotidyl transfer activity, many DNA polymerases have an editing function that removes mispaired nucleotide residues from the 3′ end of elongating primer strands, helping to ensure the fidelity of replication (for reviews, see refs *1*−*5*).

The three-dimensional structures of many DNA polymerases (DNA pols) have now been determined. Among these, the Klenow fragment (KF)[1] (*6*−*8*), T7 pol (*9*, *10*), and the homologous DNA pols from bacteriophages T4 and RB69 (*11*−*13*) have been extensively studied using steady-state and pre-steady-state kinetic methods (*14*−*26*). Detailed mechanisms for primer extension and excision of 3′-terminal nucleotide residues from the primer strand have been proposed. These mechanisms all involve two divalent metal ions which (i) orient the reactants in the proper geometry, (ii) lower the pK_a of the attacking OH group, and (iii) help to neutralize the developing negative charge on the pentacovalent transition state (*2*, *27*−*29*). All DNA polymerases with 3′−5′ exonuclease (exo) activity, whose structures are known, have a cluster of highly conserved side chains at the exo active site, including the ligands for the two divalent metal ions required for catalysis. They also have similarly positioned Tyr and Glu residues equivalent to Y323 and E116 in RB69 pol and Y497 and E357 in KF, respectively (for a compilation of conserved exo domain sequences, see refs *30*−*34*). Although the amino acid sequence of RB69 pol differs markedly from that of KF in the exo domain, the α-carbon backbone and the geometry of the metal ion ligands in the exo domain of KF and RB69 pol are nearly superimposable (*8*, *11*, *35*). Despite this close structural resemblance, the specific 3′−5′ exonuclease activity of RB69 (or T4) pol is ∼1000-fold higher than that of KF at pH 7 (*22*, *24*). To understand the basis for this difference, we have investigated the pH dependence of the exo activity of RB69 pol and some of its exo domain mutants, and compared them to that of KF (*14*, *36*, *37*). By relating our kinetic data to the crystal structures of the editing complexes of RB69 pol and KF, we provide a rationale for the difference in the exo activities of wild-type RB69 pol, its exo domain mutants, and KF.

EXPERIMENTAL PROCEDURES

Materials. The QuikChange site-directed mutagenesis kit and *Escherichia coli* strain BL21/DE3 were obtained from Stratagene Corp. (La Jolla, CA). Restriction endonucleases and T4 polynucleotide kinase were purchased from New England Biolabs. ϕ29 DNA polymerase was a gift from

† This work was supported by United States Public Health Service Grants GM54627 (W.K.) and GM28550 (C.M.J.).

* To whom correspondence should be addressed. Telephone: (203) 785-4599. Fax: (203) 785-7979. E-mail: william.konigsberg@yale.edu.

[1] Abbreviations: KF, Klenow fragment of pol I from *Escherichia coli*; HPLC, high-pressure liquid chromatography; MTEN buffer, 2-(*N*-morpholino)ethanesulfonic acid-Tris, ethanolamine, and NaCl; TBE buffer, 90 mM Tris-borate and 2 mM EDTA (pH 8.0); PT, primer−template.

10.1021/bi0302292 CCC: $27.50 © 2004 American Chemical Society
Published on Web 03/09/2004

Amersham Corp. [γ-^{32}P]ATP was also from Amersham Corp. DEAE-cellulose (DE52) and phosphocellulose were from Whatman. Source 30Q resin was obtained from Pharmacia. Electrophoresis reagents were from Bio-Rad. Other chemicals were analytical-grade. Oligonucleotides used for primers and templates were synthesized by the W. M. Keck Foundation Biotechnology Resource Laboratory (Yale University). The T4 pol structural gene was obtained from a pTL7 plasmid that we had previously reported (*24*). A plasmid, pCW19R, containing the RB69 pol structural gene was a gift from J. Karam (Tulane University, New Orleans, LA).

Construction of Mutants and Preparation of Proteins. T4 and RB69 pol mutants were constructed by PCR mutagenesis using the QuikChange site-directed mutagenesis kit (Stratagene Corp.) according to the supplier's instructions. The altered RB69 pol coding sequences were completely sequenced to verify the presence of the correct codons for the site specific substitutions and to make sure that the remaining sequence corresponded to the wild-type enzyme. The RB69 pol cDNAs were then cloned into a Bluescript expression vector downstream from the T7 promoter as previously described (*25*). The plasmids introduced into competent BL21-DE3 cells were induced with IPTG when the cell density reached an A_{590} value of 0.4. The culture was then shaken overnight at 16 °C, and the cells were harvested by centrifugation and lysed. Purification of the expressed proteins to homogeneity was accomplished using three chromatographic steps as previously described (*24*). More recently, the wild-type and mutant RB69 pol cDNAs were recloned into a pET 21b vector (Novagen Co.) so that the expressed proteins had six His residues at their C-termini. After overnight induction at 16 °C, the cells were harvested by centrifugation, lysed by sonication, and spun at high speed, and the cleared supernatant was applied to a Ni−NTA column (Novagen). After the column had been washed with sonication buffer, and then with 0.2 M imidazole in 50 mM Tris-HCl buffer (pH 8), the His_6-tagged pol was eluted with 0.5 M imidazole in the same buffer. The 0.5 M imidazole eluates were concentrated, dialyzed to remove the imidazole, and further purified on a Source 30Q column (*24*). Protein concentrations were determined by the Bradford assay and by the optical density at 280 nm using a molar extinction coefficient of 1.5×10^5 M^{-1} cm^{-1} for RB69 pol and its mutants (*24*). To test for contamination by other nucleases that would interfere with the kinetic experiments, the mutant protein preparations (5 mg/mL) were incubated with the 3′−5′ exonuclease-resistant S_p form of the 5′-^{32}P-labeled phosphorothioate primer (1 μg/mL), described below, in a Tris-HCl buffer [67 mM Tris-HCl (pH 8.8), 10 mM β-mercaptoethanol, and 60 mM NaCl] for 3 h at 25 °C. The mixture was fractionated by gel electrophoresis, and the ^{32}P-labeled degradation products were quantified using a phosphorimager (Molecular Dynamics). If we found that any of the S_p phosphorothioate substrate was degraded, we took this as an indication that the mutant DNA polymerase preparation was contaminated with exogeneous nucleases and required further purification. This was carried out by FPLC with either phosphocellulose or hydroxyapatite columns, using standard procedures (*25*).

Preparation of Substrates. Primers were labeled at their 5′-termini using [γ-^{32}P]ATP and T4 polynucleotide kinase as previously described (*38*). The R_p and S_p forms of the 17mer phosphorothioate were separated by reverse-phase HPLC according to the method of Grasby and Connolly (*39*) before being labeled with [γ-^{32}P]ATP. The eluate was dried in a Speed-Vac and redissolved in water. Duplex 3′-tailed DNA was formed by mixing equimolar amounts of the 5′-^{32}P-labeled 17mer primer (5′-CCGACCACGGAACCCCC) or the R_p form of 5′-CCGACCACGGAACCCC-sC with the 20mer template (3′-GGCTGGTGCCTTGACCCCCC) in annealing buffer [10 mM Tris-HCl, 5 mM NaCl, and 0.2 mM EDTA (pH 8.2)]. Annealing was performed by denaturing the oligonucleotide at 95 °C for 5 min and then slowly cooling the solution to 25 °C. The ^{32}P-labeled duplexes were checked by polyacrylamide gel electrophoresis followed by radioautography to ensure that all the labeled primer was in the duplex form. The DNA substrates were then stored at −20 °C.

Single-Turnover Assays for Exonuclease Activity as a Function of pH. All reactions were performed at 24 °C in a KinTek rapid quench flow instrument (model RQF-3, KinTek Corp., University Park, PA). Syringe A contained 400 nM substrate, 6 mM EDTA, and 1600 nM enzyme in 50 mM MTEN buffer [50 mM 2-(*N*-morpholino)ethanesulfonic acid-Tris, 25 mM ethanolamine, and 100 mM NaCl (adjusted to the desired pH by addition of 0.1 M HCl)] (*40*). Syringe B contained 26 mM $MgCl_2$, in MTEN buffer at the same pH as that of the solution in syringe A. Reactions were initiated by mixing equal volumes (16 μL) of these two samples driven by the MTEN buffer at the same pH as that of the solutions in each syringe. The reaction was quenched at various times by the addition of EDTA (0.5 mM, pH 8.0). For some mutants, for which the reactions were slower than those catalyzed by the wild-type enzyme, assays were performed manually using the same conditions. The mixtures from the quenched reactions were collected in Eppendorf tubes, and then aliquots were removed and analyzed by polyacrylamide gel electrophoresis (20% polyacrylamide and 50% urea in TBE buffer) and quantified using a phosphorimager as previously described (*26*). In some experiments, with wild-type RB69 pol, the order of mixing was altered. When the enzyme was present in syringe A, and the substrate together with $MgCl_2$ was added from syringe B, the observed excision rate was slower than when the substrate and enzyme were both present in syringe A and $MgCl_2$ was added from syringe B. In some experiments, we doubled the enzyme concentration but found no change in the excision rate. We used MTEN because it is a suitable buffer for studying reactions between pH 6.5 and 8.5 as it maintains a constant ionic strength in this range (*40*). Exo rates obtained below pH 6 are unreliable due to irreversible inactivation of RB69 pol over time. For example, when we incubated RB69 pol at pH 5.5 in 0.1 M sodium acetate buffer at 24 °C, taking aliquots at various times, adjusting the pH to 7 with MTEN buffer, and assaying for exo activity, the observed rates decreased with a longer exposure of the enzyme at pH 5.5. At pH >9.5, RB69 pol, its mutants, and KF exhibited lower exo activity presumably because the Mg^{2+} concentration is reduced to <15 mM [K_{sp} for $Mg(OH)_2 = 1.8 \times 10^{-11}$], the optimum concentration for excision.

Data Analysis. Data from single-turnover experiments were fit to a single-exponential equation using Sigma Plot version 4.14 (Jandel Scientific, San Rafael, CA).

Table 1: Excision Rate Constants (k_{exo}) as a Function of pH, Determined under Single-Turnover Conditions[a]

	k_{exo} (s^{-1})				
enzyme	pH 6.5	pH 7.0	pH 7.5	pH 8.0	pH 8.5
RB69 pol	3.0	5.0	6.6	7.7	8.1
RB69 E116A	3.9×10^{-5}	11×10^{-5}	2.8×10^{-4}	7.5×10^{-4}	5.3×10^{-4}
RB69 K302A	1.1×10^{-3}	3.3×10^{-3}	1.0×10^{-2}	3.2×10^{-2}	0.11
RB69 Y323F	5.6×10^{-4}	1.8×10^{-3}	5.8×10^{-3}	1.9×10^{-2}	5.6×10^{-2}
RB69 K302A/Y323F	2.1×10^{-5}	6.5×10^{-5}	2.0×10^{-4}	6.4×10^{-4}	2.0×10^{-3}
KF	1.7×10^{-3}	5.4×10^{-3}	1.6×10^{-2}	5.2×10^{-2}	0.16

[a] Final concentrations: 800 nM enzymes, 200 nM substrate, and 10 mM Mg^{2+}. Precision ± 15%. All reactions were carried out at 24 °C in MTEN buffer which contains 50 mM 2-(*N*-morpholino)ethanesulfonic acid, 25 mM tris(hydroxymethyl)aminomethane, 25 mM ethanolamine, and 100 mM sodium chloride. The pH was adjusted to the stated value with 0.1 M HCl. Reactions were quenched with 400 mM EDTA.

Table 2: Elemental Effects for Wild-Type and Mutant RB69, T4 Pols, and KF[a]

	k_{exo} (s^{-1})		
enzyme	3′-tailed duplex all-oxygen substrate	3′-tailed duplex phosphorothioate	k_{exo} ratio (O/S)[b]
RB69 pol	24	17	1.4
T4 pol	130	91	1.4
RB69 K302A	0.10	2.0×10^{-2}	5
T4 K299A	0.18	5.0×10^{-2}	4
RB69 Y323F	0.14	1.2×10^{-3}	117
T4 Y320F	0.12	9.6×10^{-4}	121
T4 Y320A	7.5×10^{-2}	8.5×10^{-3}	9
RB69 K302A/Y323F	1.3×10^{-2}	8.1×10^{-4}	16
T4 K299A/Y320F	1.3×10^{-2}	5.0×10^{-4}	26
KF	0.33	2.0×10^{-2}	16
KF Y497F	4.1×10^{-3}	3.5×10^{-4}	12

[a] Final concentrations: 600 nM enzymes, 150 nM substrates, 10 mM Mg^{2+}, and 67 mM buffer [Tris-HCl (pH 8.8), 10 mM β-mercaptoethanol, and 60 mM NaCl]. Reactions were carried out at 24 °C and quenched with 400 mM EDTA. Precision ±15%. [b] Ratio of the k_{exo} values for the substrate with the all-oxygen 3′-terminal phosphodiester to the k_{exo} for the 3′-terminal phosphorothioate.

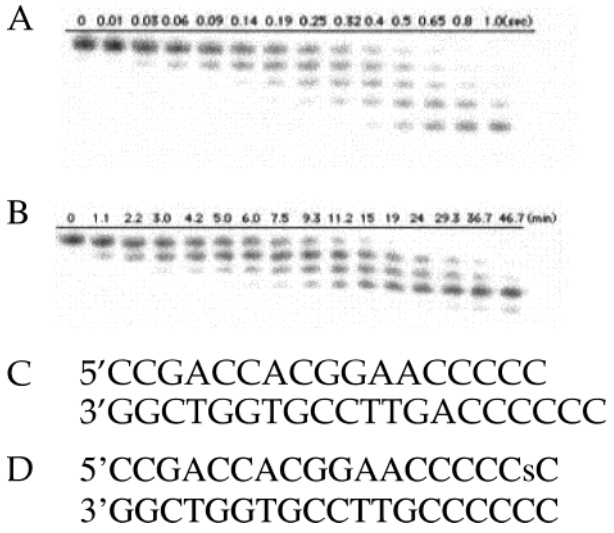

FIGURE 1: Digestion patterns visualized and quantified by phosphorimaging of urea−acrylamide gels that were loaded with timed aliquots from rapid chemical quench experiments designed to measure the rate of 3′−5′ exonuclease digestion of 5′-^{32}P-labeled substrates shown in panels C and D by (A) RB69 DNA pol and (B) KF. Reactions were carried out in MTEN buffer at pH 7.0 and 24 °C. The reaction times prior to the quench are given above the solid lines. Note that the time is seconds in panel A and minutes in panel B. The reaction conditions are described in Experimental Procedures and in the legend of Figure 2. (C) All-oxygen substrate, 17/20mer 3′-tailed duplex. (D) Sulfur-substituted (R_pS) substrate, 17/20mer 3′-tailed phosphorothioate duplex.

RESULTS

pH−Activity Profiles of KF, T4, and RB69 Pols. We began this study using T4 pol since a complete kinetic scheme (*22*), pH−activity profiles (*41*), and a considerable amount of kinetic data for its exo activity had already been reported (*22*−*24*). Although a crystal structure had been determined for the exo domain of T4 pol (*35*), the structure of intact T4 pol has not been determined. Crystal structures of the closely related RB69 pol have been determined in three different forms, the apoenzyme (*11*); the editing mode, in a complex with a primer−template (PT) (*12*); and the pol mode in a ternary complex with a dideoxy-terminated PT and a complementary incoming dNTP (*13*). When the crystal structure of the RB69 pol editing complex was reported, we focused all our efforts on this enzyme so that we could relate kinetic parameters for the exo reaction to the structure of the RB69 pol−PT complex (*12*). Because the exo domains of T4 and RB69 pols are almost superimposable (*11*, *35*), we expected that kinetic results obtained with RB69 and T4 pols would be nearly identical; however, the excision rates, determined under single-turnover conditions in Tris buffer, were ∼5-fold higher for T4 pol than for RB69 pol (Table 2). With T4 pol, we obtained k_{exo} values close to those reported by Capson *et al*. (*22*). The excision rates we observed with both T4 and RB69 pol were almost identical when the reaction was carried out in MTEN buffer. For brevity, we report only data obtained for RB69 pol and its mutants on pH versus activity; however, we present results for both RB69 and T4 pol as well as their mutants for experiments with the phosphorothioates to further support some of the conclusions drawn from this part of the study on the elemental effect.

To investigate the striking difference in exo activity between RB69 pol and Klenow fragment (KF), we first examined the pH−exonuclease activity profiles of RB69 pol and KF under single-turnover conditions. For substrates, we used 5′-^{32}P-labeled 17/20mers with four mismatched C residues, and an identical 17/20mer with a phosphorothioate linkage at its 3′-terminus (Figure 1C,D). Double-stranded, 3′-mismatched substrates have an affinity (K_d ∼ 70 nM) (*22*) higher than the K_m for single-stranded (ss) DNA substrates (∼10 μM) (*24*), facilitating pre-steady-state kinetic studies. The four unpaired nucleotides at the 3′-terminus are sufficiently long to extend into the exonuclease active site even when the dsDNA substrate is bound initially in the pol mode (*12*, *13*, *42*). It was our expectation that, with a 3′-frayed mismatched primer, the additional complexity in interpreting

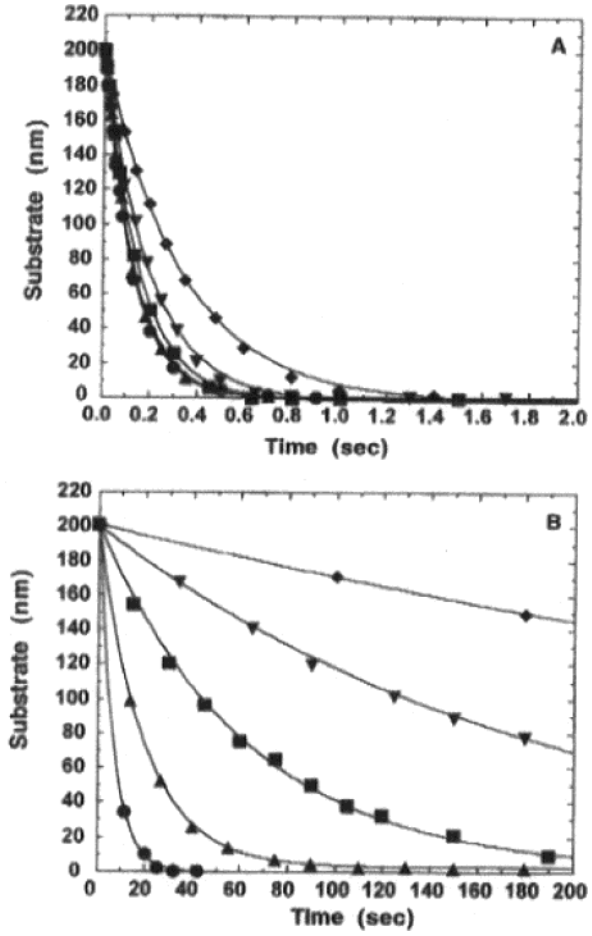

FIGURE 2: Single-turnover assays for the exonuclease activity of (A) RB69 polymerase and (B) KF. All reactions were carried out in 50 mM MTEN buffer at pH 6.5 (●), 7.0 (▲), 7.5 (■), 8.0 (▼), and 8.5 (◆) at 24 °C. The reaction mixture contained 200 nM 5′-^{32}P-labeled 3′-tailed 17/20 mer substrate, 800 nM enzyme, and 10 mM $MgCl_2$.

kinetic results, which include duplex melting and partitioning of the substrate between the exo and pol modes, could be avoided (*22*, *41*, *42*).

A typical digestion pattern obtained for nucleotide excision by wild-type RB69 pol and KF at pH 7.0 is shown in panels A and B of Figure 1. At this pH, there was a large difference in excision rates between the two enzymes. The decrease in the intensity of the labeled primer band for both RB69 pol and KF (Figure 2) as a function of time fit an exponential decay curve, indicating that we were measuring the rate of a single process. When we determined the exo activity of RB69 and T4 pol as a function of pH between pH 6.5 and 8.5, the slope of log(activity) versus pH was close to 0 for both enzymes (Figure 3). We also examined the pH versus exo activity of another B family DNA polymerase, ϕ29 pol, the overall sequence of which is only slightly similar to that of RB69 pol except for well-defined motifs, some of which are in the exo domains, where the sequences are identical (*11*, *43*, *44*). The ϕ29 pol also displayed the same pH−activity profile as RB69 pol, suggesting that this behavior might be a general feature of B family DNA pols that have exo activity. By contrast, KF had a log-linear pH profile with a slope of 1 (Figure 3). There are a few points about the exo rates that are worth noting. (i) Buffer systems have a marked influence on the values of k_{exo}. For example, at pH 8.5, the

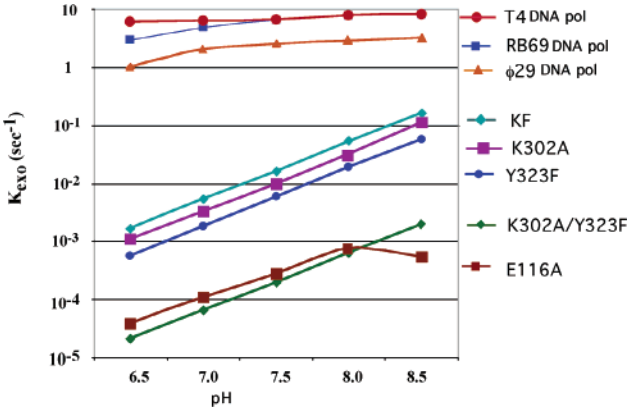

FIGURE 3: Excision rates (k_{exo}) vs pH for T4 pol, RB69 pol, and four of its exo domain mutants (K302A, Y323F, K302A/Y323F, and E116A). The pH vs excision rates for ϕ29 pol and KF are also presented. Assays were carried out under single-turnover conditions with a 3′-tailed DNA duplex (17/20mer) having a four-base mismatch at the 3′-terminus (Figure 1C). Reaction conditions are given in the footnotes of Table 1, the legend of Figure 2, and Experimental Procedures.

k_{exo} for RB69 pol is 8 s^{-1} in MTEN buffer (Table 1), but at pH 8.8, the k_{exo} is 24 s^{-1} in Tris-HCl buffer (Table 2). (ii) Similar differences in k_{exo} for T4 pol were observed in these two buffer systems, but the k_{exo} value of 130 s^{-1} in Tris-HCl buffer (pH 8.8) (Table 2) is in good agreement with the k_{exo} of 100 s^{-1} reported by Capson *et al.* (*22*) under similar conditions. The influence of different buffer systems on the exo rates of T4 pol has also been recorded (*41*). (iii) In contrast to the wild-type enzymes, the exo domain mutants of T4 and RB69 pol had similar k_{exo} values in Tris-HCl buffer (pH 8.8) (Table 2).

Klenow Fragment and the Exo Domain Mutants of RB69 Pol Have Similar pH−Activity Profiles. To further explore the basis for the difference in exo activity between RB69 pol and KF, we examined the pH−exo activity profiles of three single site mutants of RB69 pol (K302A, Y323F, and E116A) as well as a double mutant (K302A/Y323F). These residues were chosen because (i) K302 is a highly conserved residue near the catalytic site in the exo domains of the B family but has no equivalent in the family A DNA polymerases (*11*, *43*, *44*), (ii) Y323 is also highly conserved in the exo domains of both A and B family DNA polymerases and the equivalent Tyr residue, Y497 in KF, participates directly in the excision reaction (*7*, *29*, *45*, *46*), and (iii) E116 was also examined because its side chain points toward the exo active center (*12*) and its carboxylate group may be involved indirectly in catalysis like the corresponding E357 residue in KF (*2*, *14*, *27*, *45*, *46*).

All of the RB69 pol mutants with single-site substitutions (K302A, Y323F, and E116A) had k_{cat} values lower than that of the wild type for degradation of $p(dC)_{10}$ and $p(dT)_{16}$ under steady-state conditions where the substrates were present in 8-fold molar excess over the enzyme (data not shown). To determine whether the effect of each of these mutants on the exo activity was additive, we tested the double mutant K302A/Y323A for its exo activity, along with the corresponding single-site mutants and KF, as a function of pH, under single-turnover conditions. The assays were performed with the enzymes and 17/20mer substrates at concentrations 3 times higher than the estimated K_d for the enzyme−substrate complexes (*22*). The results in Table 1 and Figure

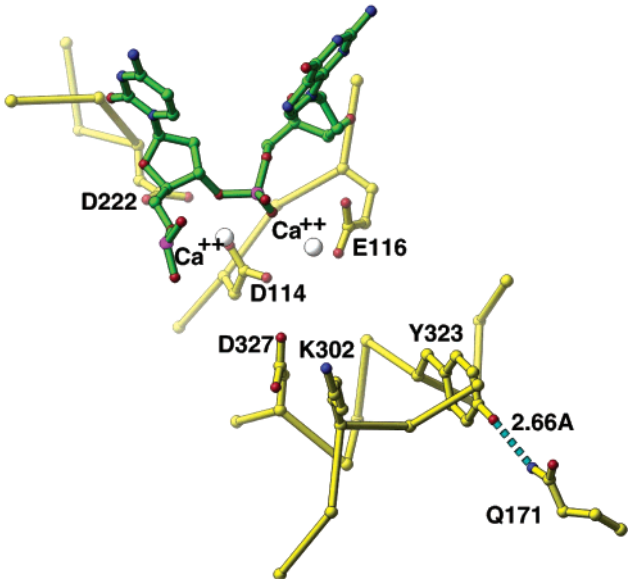

FIGURE 4: Model of the exo active site of RB69 pol complexed with a PT in the exo mode based on the 2.7 Å structure determined by Shamoo and Steitz (*12*) (PDB entry 1CLQ). The dinucleotide substrate is in green, and the protein is in yellow. The orientation and the distance (2.66 Å) between the γ-hydroxyl group of Y323 and the amide nitrogen of Q171 are shown. The blue dots represent the potential for hydrogen bonding. The structure has Ca^{2+} in place of Mg^{2+}, and the protein in this form has no exonuclease activity. Although the distance is not indicated, K302 in this structure is disordered and is further from the active site than in other exo mode structures of RB69 and T4 pols (*11*, *35*).

3 show that there was very little change in the k_{exo} for wild-type RB69 pol between pH 6.5 and 8.5, whereas for KF and for the four RB69 pol mutants, the exo activity was much lower than that of wild-type RB69 pol at all pH values that were studied. The plots of log k_{exo} versus pH for KF and for nearly all of the RB69 pol mutants were parallel with a slope of 1, in contrast to the very shallow slope of the plot for wild-type RB69 pol. The E116A mutant exhibited somewhat aberrant behavior at the higher end of the pH range that we cannot interpret at present. The k_{exo} values for the K302A and Y323F RB69 pol mutants were only slightly lower than the k_{exo} for KF, whereas the k_{exo} values for E116A and the double mutant K302A/Y323F were ~100 times lower than that of KF and 10 000 times lower than that of wild-type RB69 pol at pH 8.5.

A Mutant in the Exo Domain that Enhances the Exo Activity of RB69 Pol. On the basis of the structure of the exo mode complex of a PT and RB69 pol (*12*), where Y323 is in a position to form a hydrogen bond to the side chain amide group of Q171 (Figure 4), we produced a Q171A variant that had a k_{exo} of 130 s^{-1}, a value 5 times higher than that of wild-type RB69 pol, when assayed in Tris-HCl buffer (pH 8.8), but identical to the k_{exo} for T4 pol (Table 2).

Effect of Phosphorothioates on the Excision Rates. Substrates with a sulfur substitution in place of a nonbridging oxygen in the terminal phosphodiester (phosphorothioates) have been used to estimate the elemental effect for exonuclease reactions of pols (*36*, *46*−*49*). An increase in the elemental effect [the ratio of k_{exo} for all-oxygen substrates vs k_{exo} for 3′-terminal phosphorothioates (designated as O/S)] has often been interpreted to mean that chemistry has become rate-limiting. All the phosphorothioates used in this study were R_p stereoisomers, the only form degraded by the DNA polymerases that have been examined (*36*, *47*−*49*). To ensure that differences in the O/S ratios were due to changes in k_{exo} rather than K_d, we used two different enzyme concentrations (one twice the other) while keeping the amount of thio-substituted PTs constant in experiments with the RB69 pol mutants shown in Table 2 and obtained identical O/S ratios. The O/S ratios for excision by T4 and RB69 pols were both 1.4 (Table 2). By contrast, KF had an O/S ratio of 16. The replacement of K299 in T4 and the equivalent residue, K302, in RB69 pol with Ala gave nearly identical O/S ratios (~5). Replacement of Y320 with Ala in T4 pol resulted in an increase in the O/S ratio to 9. The double mutant, where both the Lys and Tyr residues were replaced with Ala, gave an O/S ratio of 26, a value somewhat greater than the O/S ratio of 16 for the RB69 pol K302A/Y323F double mutant and the O/S ratio of 16 for KF (Table 2). A curious finding was that the O/S ratios for the Y323F mutant in RB69 pol and the corresponding mutant, Y320F in T4 pol, were more than 100. By contrast, when the equivalent conserved Tyr (Y497) in KF was replaced with Phe, the O/S ratio was similar to that of wild-type KF (Table 2).

DISCUSSION

The goal of this study was to provide a rationale for the dramatically enhanced levels of 3′−5′ exonucleolytic activity exhibited by RB69 pol relative to KF (*2*, *22*, *24*, *48*). Given the striking similarity between the overall tertiary structures of the exo domains in RB69 pol (*11*−*13*) and KF (*2*, *6*, *8*, *27*), there was no obvious structural element that could account for the difference in activity except for a strategically placed Lys (residue 302 in RB69 pol). This residue is highly conserved in B family DNA polymerases that have exo activity but is absent in the A family DNA polymerases. Accordingly, we targeted this Lys residue for replacement with Ala with the hope that the kinetic behavior of the K302A mutant would help in explaining the 1000-fold difference in exo activity between the two enzymes. We also replaced other conserved residues whose side chains were oriented toward the exo active site, but we excluded acidic residues that were known to be ligands for the two divalent metal ions in the exo active site (*12*, *41*).

pH−*Activity Profiles.* We first decided to examine the exo activity of wild-type and mutant RB69 pols and KF as a function of pH, since previous studies on the pH−activity profiles of T4 pol (*41*) and KF (*14*) indicated that their behavior differed greatly. Although we assumed that RB69 pol would have a pH−activity profile like that of T4 pol, we chose to check its pH−activity profile to verify this supposition. By performing these experiments using a single buffer system suitable for pHs ranging from pH 6.5 to 8.5, we avoided problems that occur when buffer systems are changed during the experiment to maintain optimal buffering capacity. We found no evidence for the two pH optima reported for T4 pol (*41*). Instead, we found that nucleotide excision by RB69 pol was insensitive to pH, and was much faster than the reaction catalyzed by KF, suggesting that a step prior to chemistry is rate-limiting. The pH−activity profile that we obtained for KF was similar to that reported by Derbyshire *et al*. (*14*). As argued elsewhere (*36*, *50*), chemistry is most probably rate-limiting for the exo reaction,

so the pH profile represents the pH dependence of the chemical step. The observation that site specific substitutions in the exo domain of RB69 pol both reduced the specific exo activity and altered the flat pH−activity profile to one that resembled that of KF strongly implies that the rate-limiting step of the reaction catalyzed by these RB69 pol variants was altered. Two of these residues, K302 and Y323, appear to be crucial for the rate enhancement of RB69 pol relative to KF. When mutants having substitutions at these two positions are combined, the double mutant (K302A/Y323F) also behaves like KF, but its specific exo activity is much lower than that found with the polymerase having single-site replacements, suggesting that combining the two substitutions has an additive effect on the reduction of exo activity.

Effect of Sulfur Substitution on Excision Rates. Measurements of sulfur elemental effects can also serve as a diagnostic for a rate-limiting chemical step, and these data support the conclusions derived from our pH studies. Wild-type T4 and RB69 pols show essentially no elemental effect on the exonuclease reaction, and this, like the flat pH−activity profile, suggests that a step other than chemistry is rate-limiting. By contrast, wild-type KF, where the available evidence indicates rate-limiting chemistry (see above), has an elemental effect of 16 (this work and ref *46*), and several of the T4 and RB69 pol mutants have elemental effects in the range of 4−26. Again, this correlates with the pH−activity profiles for the corresponding proteins and is consistent with a rate-limiting chemical step. The magnitudes of the elemental effects observed for KF and these mutant proteins are close to the range (4−11-fold) reported by Herschlag *et al*. for the nonenzymatic cleavage of a model phosphodiester (*51*). This could indicate that the enzymatic reaction at the exonuclease active site is affected solely by the electronic differences between the oxygen- and sulfur-containing phosphate reaction centers. Alternatively, the similar numbers could be largely coincidental, given that the restricted space within an enzyme active site may result in steric problems when processing the sulfur-substituted substrate.

Steric effects indeed play a significant role in the structural explanation offered by Brautigam and Steitz for the elemental effect at the KF 3′−5′ exonuclease active site (*46*). They observed a strong hydrogen bond (interatomic distance of 2.6 Å) between the γ-hydroxyl group of Y497 and the pro-R_p oxygen of a DNA substrate bound at the exonuclease site. This suggested that the γ-hydroxyl group of Tyr helps to correctly position the substrate for hydrolysis, consistent with the 62-fold drop in activity when this Tyr is replaced with Phe (*14*). When a sulfur atom was in the R_p position, replacing oxygen, both the sulfur and the γ-hydroxyl group of Y497 were pushed away from each other by 1 Å, resulting in a displacement of the scissile phosphorus atom by 0.67 Å (Figure 5). The fact that the kinetics can be rationalized on the basis of displacement of the scissile phosphorus is in agreement with the proposal that chemistry is the rate-determining step.

Further support for the idea that the sulfur elemental effect may have a substantial steric component is provided by the 120-fold elemental effects observed with the RB69 pol Y323F mutant and the homologous Y320F mutant of T4 pol. These extremely large elemental effects correlate with the presence of an aromatic side chain at residue 323 (RB69 pol) or 320 (T4 pol), together with the active site lysine (K302 of RB69 pol or K299 of T4 pol). When the active site lysine is mutated to alanine, or is absent in the wild-type protein (as in KF), the elemental effect is ~10-fold lower. Thus, the large elemental effects probably result from extreme steric crowding in the transition state for hydrolysis of the sulfur-containing substrate. A logical inference from this reasoning is that the hydrolysis of the sulfur-containing substrate by wild-type T4 and RB69 pols also proceeds through a sterically crowded transition state; however, because the chemical step is so much faster, the results of an even 100-fold decrease in rate are kinetically invisible. An analogous correlation between sulfur elemental effects and the size of an active site side chain has been observed at the polymerase active site of KF (*52*).

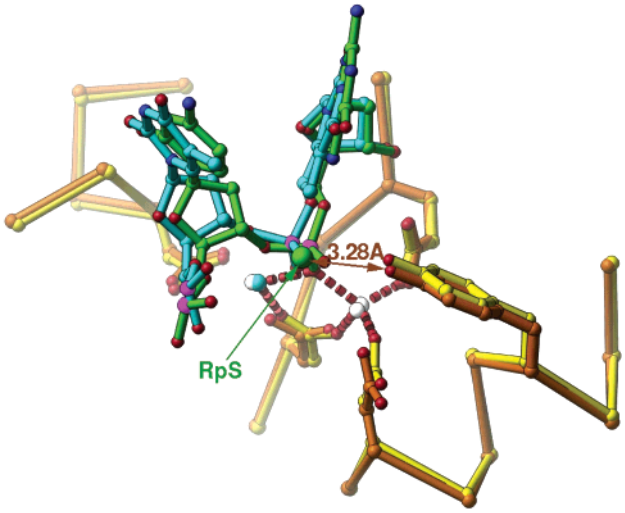

FIGURE 5: Least-squares superposition of the KF exo active site−substrate complexes (*46*). The R_pS−substrate complex is green, and the protein is yellow. For the all-oxygen complex, the substrate is green but the pro-R_p oxygen is red (partially hidden under the arrowhead) and the protein is brown. The divalent ions in the A (white) and B (blue-white) sites are shown connected to their liganding groups by red dots (see Figures 5 and 6 in ref *46* for further details). The distance between the R_pS (in green) and the γ-hydroxyl oxygen of Y497 is 3.28 Å, an increase of 0.6 Å compared to the distance between the pro-*R* oxygen and the γ-hydroxyl oxygen of Y497 in the all-oxygen substrate−KF complex (*46*).

Relationship between the Structures of KF and RB69 Pol−Oligonucleotide Complexes and the Rates of the Exo Reaction. In RB69 pol, residues K302 and Y323, perhaps acting in concert, enhance the rate of the chemical step so that it is no longer limiting. Since water is the source of the nucleophile (hydroxide ion), then activation of water by the divalent metal ion in the A site would be required at the exo active site (*2*, *29*). In addition, orienting the water molecule or nascent hydroxide ion so that it is optimally positioned for in-line attack is expected to be a crucial function of the metal ion in the A site, based on analogy with KF (*7*, *8*). The Y323 OH group may contribute a bifurcated hydrogen bond to the hydroxide ion and to the pro-R_p oxygen as proposed for KF (see Figure 6 in ref *46*). These interactions, together with a hydrogen bond from E116, would help to properly position the phosphodiester bond for hydrolysis and to orient the attacking hydroxide ion (derived from the water molecule in the active site) prior to hydrolysis of the scissile phos-

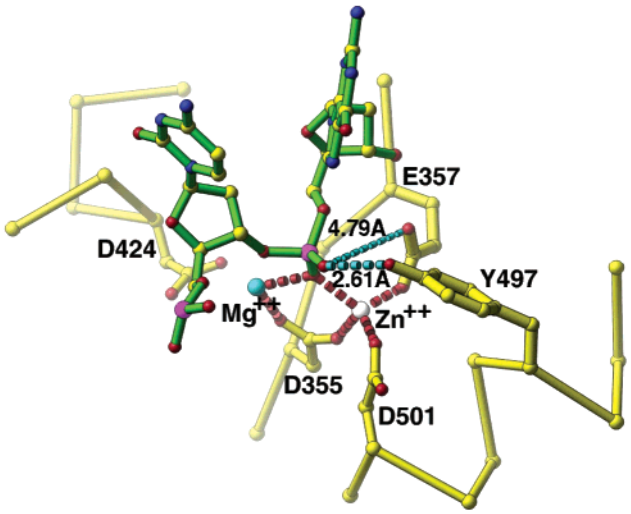

FIGURE 6: Active site region of KF (yellow) (*46*) bound to the all-oxygen DNA substrate (green). Hydrogen bonds to the pro-R_p oxygen from the carboxyl group of E357 and the γ-hydroxyl group of Y497 are shown as blue dots. Ligands to the Mg^{2+} and Zn^{2+} metal ions are shown as red dots.

phodiester bond. It is also possible that the Y323 side chain might help to position the frayed single-stranded DNA in a strained conformation that would accelerate excision of the nucleotide residue at the 3′-terminus as suggested for the analogous situation with KF (*50*). The corresponding residues in KF, E357 and Y497, also appear to play important roles in keeping the substrate properly oriented for in-line attack by the hydroxide ion (Figure 6) (*7*, *8*). Replacement of either of these residues with Ala significantly reduces the hydrolytic rate but does not fully abolish the exo activity (*14*). The metal ion in the A site also aligns the pro-S_p oxygen in the phosphodiester linkage so that it is close to a position that it would occupy in the pentacovalent transition state (see Figures 1 and 2 in ref *46*).

The role proposed for the B metal ion is consistent with all of the structures and with the kinetic parameters for KF; however, for RB69 pol, metal ion B is likely to be assisted in stabilizing the developing negative charges in the transition state by the positively charged ϵ-amino group of K302 in RB69 pol, presumably resulting in substantial acceleration of the hydrolytic reaction so that a step preceding chemistry now limits the excision rate (*2*). It should be noted that the side chain of K302 is disordered in the exo mode complex (*12*), perhaps because calcium rather than magnesium ions were present in this structure. Since Ca ions have a larger ionic radius than Mg ions, the local stereochemistry in the exo active site was probably perturbed and could account for the fact that this complex was devoid of activity. On the other hand, in the 5 Å structure of the RB69 pol−ssDNA complex, the ϵ-amino group of K302 is ~3 Å from the nonbridging oxygen of the scissile phosphate (*11*). The same distance (3 Å) between the K299 amino group and the relevant phosphate oxygen was also observed in the T4 pol N388 exo domain in a complex with ssDNA (*35*). Both of these structural results support the notion that this lysine residue is an important feature of the exo catalytic site in T4 and RB69 pol.

Because we have used a frayed 3′-PT where the ss primer is sufficiently long to reach the exo active site (*42*), it is unlikely that DNA melting would limit the exo rate for wild-type T4 and RB69 pols. The following possibilities for the rate-determining step should be considered. (i) The rate of binding of the frayed PT to the enzyme might be limiting. (ii) The rate may be limited by the time required for the frayed single-stranded region at the 3′-end of a mismatched PT to attain the optimal geometry in the exo active site after addition of Mg^{2+}. (iii) After addition of Mg^{2+}, the orientation of some of the metal ion ligands in the protein may require some time to adjust to a conformation that would facilitate catalysis. The rate of this putative adjustment would be expected to be slower than the rate of diffusion of a divalent cation into the active site and slower than the chemical step which should be very rapid if the geometry of the ground state closely resembles that of the transition state of the enzyme−substrate complex (*2*, *51*).

Another feature of RB69 pol that may be relevant in explaining the rapid exo rate is the flexibility of the Y323 side chain. In one of the crystal structures (*12*), residue Y323 points away from the active site and the Tyr OH group is hydrogen bonded to the side chain amide nitrogen of Q171 (Figure 4). Before a catalytically relevant structure can be assumed, this hydrogen bond must be broken. This is likely to happen because another crystal form of RB69 pol (*13*) shows Y323 in a different position where it can potentially form a hydrogen bond to the pro-R_p oxygen of the substrate. When we determined the excision rate of the Q171A derivative of RB69 pol, we found that it was 5 times faster than that of the wild-type enzyme. It is worth noting that T4 pol has an Asp residue at the position equivalent to Q171 in RB69 DNA and that the k_{exo} for T4 pol is ~6 times higher than that for RB69 pol. It is tempting to speculate that, because of this difference, there is a longer residence time for Y320 (in T4 pol) in an orientation where it points toward the active site compared to the situation with Y323 (in RB69 pol).

The pH−activity profiles for KF and the RB69 pol exo mutants assume that hydroxide ions can be freely exchanged with the solvent either directly or via proton transfer. This is consistent with the analysis of phosphodiester bond hydrolysis by KF reported by Fothergill *et al*. (*28*) using the electron valence bond method to evaluate the contributions of the two metal ions to the hydrolytic mechanism. According to Fothergill *et al*. (*28*), the main role of metal ion A is to electrostatically stabilize the attacking hydroxide ion. This notion is still in agreement with a role for metal ion A in correctly aligning the reactants and lowering the pK_a of an attacking water molecule in the active site as suggested by Steitz and Steitz (*29*). The evaluation of these subtle features of the exo mechanism will require further structural information. In particular, a high-resolution crystal structure of a complex poised for excision would clarify some of the uncertainties that remain about the exo reaction catalyzed by RB69 pol.

With the demonstration of the remarkable divergence in the pH profiles and kinetic schemes for the exo reaction, between KF and RB69 pol as well as other B family DNA polymerases, the question of the possible biological significance of these differences arises. A conceivable rationale is that replicative DNA polymerases must rapidly and faithfully copy long stretches of DNA which demands efficient removal of mismatched nucleotide residues. This editing requirement is not as stringent for repair polymerases such as KF because

they copy shorter lengths of DNA at slower rates. Thus, the probability of incorporating mispaired bases into the genome would be lower; consequently, DNA polymerases having a repair role would not need an exo activity as potent as that of replicative polymerases.

ACKNOWLEDGMENT

We thank Ranjini Sundaram for construction of some of the T4 and RB69 pol mutants. We are grateful to Jim Karam for the RB69 pol cDNA. We also have appreciated helpful discussions with T. C. Lin, and we thank Liz Vellali for skillful preparation of the manuscript.

REFERENCES

1. Joyce, C. M., and Steitz, T. A. (1994) Function and structure relationships in DNA polymerases, *Annu. Rev. Biochem. 63*, 777−822.
2. Brautigam, C. A., and Steitz, T. A. (1998) Structural and functional insights provided by crystal structures of DNA polymerases and their substrate complexes, *Curr. Opin. Struct. Biol. 8*, 54−63.
3. Steitz, T. A. (1999) DNA polymerases: structural diversity and common mechanisms, *J. Biol. Chem. 274*, 17395−17398.
4. Patel, P. H., Suzuki, M., Adman, E., Shinkai, A., and Loeb, L. A. (2001) Prokaryotic DNA polymerase I: evolution, structure, and "base flipping" mechanism for nucleotide selection, *J. Mol. Biol. 308*, 823−837.
5. Kunkel, T. A., and Bebenek, K. (2000) DNA replication fidelity, *Annu. Rev. Biochem. 69*, 497−529.
6. Ollis, D. L., Brick, P., Hamlin, R., Xuong, N. G., and Steitz, T. A. (1985) Structure of large fragment of *Escherichia coli* DNA polymerase I complexed with dTMP, *Nature 313*, 762−766.
7. Beese, L. S., Derbyshire, V., and Steitz, T. A. (1993) Structure of DNA polymerase I Klenow fragment bound to duplex DNA, *Science 260*, 352−355.
8. Freemont, P. S., Friedman, J. M., Beese, L. S., Sanderson, M. R., and Steitz, T. A. (1988) Cocrystal structure of an editing complex of Klenow fragment with DNA, *Proc. Natl. Acad. Sci. U.S.A. 85*, 8924−8928.
9. Doublie, S., Tabor, S., Long, A. M., Richardson, C. C., and Ellenberger, T. (1998) Crystal structure of a bacteriophage T7 DNA replication complex at 2.2 Å resolution, *Nature 391*, 251−258.
10. Doublie, S., and Ellenberger, T. (1998) The mechanism of action of T7 DNA polymerase, *Curr. Opin. Struct. Biol. 8*, 704−712.
11. Wang, J., Sattar, A. K., Wang, C. C., Karam, J. D., Konigsberg, W. H., and Steitz, T. A. (1997) Crystal structure of a pol alpha family replication DNA polymerase from bacteriophage RB69, *Cell 89*, 1087−1099.
12. Shamoo, Y., and Steitz, T. A. (1999) Building a replisome from interacting pieces: sliding clamp complexed to a peptide from DNA polymerase and a polymerase editing complex, *Cell 99*, 155−166.
13. Franklin, M. C., Wang, J., and Steitz, T. A. (2001) Structure of the replicating complex of a pol alpha family DNA polymerase, *Cell 105*, 657−667.
14. Derbyshire, V., Grindley, N. D., and Joyce, C. M. (1991) The 3′−5′ exonuclease of DNA polymerase I of *Escherichia coli*: contribution of each amino acid at the active site to the reaction, *EMBO J. 10*, 17−24.
15. Eger, B. T., Kuchta, R. D., Carroll, S. S., Benkovic, P. A., Dahlberg, M. E., Joyce, C. M., and Benkovic, S. J. (1991) Mechanism of DNA replication fidelity for three mutants of DNA polymerase I: Klenow fragment KF(exo+), KF(polA5), and KF(exo−), *Biochemistry 30*, 1441−1448.
16. Dahlberg, M. E., and Benkovic, S. J. (1991) Kinetic mechanism of DNA polymerase I (Klenow fragment): identification of a second conformational change and evaluation of the internal equilibrium constant, *Biochemistry 30*, 4835−4843.
17. Kuchta, R. D., Mizrahi, V., Benkovic, P. A., Johnson, K. A., and Benkovic, S. J. (1987) Kinetic mechanism of DNA polymerase I (Klenow), *Biochemistry 26*, 8410−8417.
18. Kuchta, R. D., Benkovic, P., and Benkovic, S. J. (1988) Kinetic mechanism whereby DNA polymerase I (Klenow) replicates DNA with high fidelity, *Biochemistry 27*, 6716−6725.
19. Donlin, M. J., Patel, S. S., and Johnson, K. A. (1991) Kinetic partitioning between the exonuclease and polymerase sites in DNA error correction, *Biochemistry 30*, 538−546.
20. Wong, I., Patel, S. S., and Johnson, K. A. (1991) An induced-fit kinetic mechanism for DNA replication fidelity: direct measurement by single-turnover kinetics, *Biochemistry 30*, 526−537.
21. Johnson, K. A. (1993) Conformational coupling in DNA polymerase fidelity, *Annu. Rev. Biochem. 62*, 685−713.
22. Capson, T. L., Peliska, J. A., Kaboord, B. F., Frey, M. W., Lively, C., Dahlberg, M., and Benkovic, S. J. (1992) Kinetic characterization of the polymerase and exonuclease activities of the gene 43 protein of bacteriophage T4, *Biochemistry 31*, 10984−10994.
23. Wu, P., Nossal, N., and Benkovic, S. J. (1998) Kinetic characterization of a bacteriophage T4 antimutator DNA polymerase, *Biochemistry 37*, 14748−14755.
24. Lin, T. C., Karam, G., and Konigsberg, W. H. (1994) Isolation, characterization, and kinetic properties of truncated forms of T4 DNA polymerase that exhibit 3′−5′ exonuclease activity, *J. Biol. Chem. 269*, 19286−19294.
25. Yang, G., Lin, T., Karam, J., and Konigsberg, W. H. (1999) Steady-state kinetic characterization of RB69 DNA polymerase mutants that affect dNTP incorporation, *Biochemistry 38*, 8094−8101.
26. Yang, G., Franklin, M., Li, J., Lin, T. C., and Konigsberg, W. (2002) A conserved Tyr residue is required for sugar selectivity in a Pol alpha DNA polymerase, *Biochemistry 41*, 10256−10261.
27. Beese, L. S., and Steitz, T. A. (1991) Structural basis for the 3′−5′ exonuclease activity of *Escherichia coli* DNA polymerase I: a two metal ion mechanism, *EMBO J. 10*, 25−33.
28. Fothergill, M. D., Goodman, M. F., Petruska, J., and Warshel, A. (1995) Structure-Energy Analysis of the Role of Metal Ions in Phosphodiester Bond Hydrolysis by DNA Polymerase I, *J. Am. Chem. Soc. 117*, 11619−11627.
29. Steitz, T. A., and Steitz, J. A. (1993) A general two-metal-ion mechanism for catalytic RNA, *Proc. Natl. Acad. Sci. U.S.A. 90*, 6498−6502.
30. Bernad, A., Blanco, L., Lazaro, J. M., Martin, G., and Salas, M. (1989) A conserved 3′−5′ exonuclease active site in prokaryotic and eukaryotic DNA polymerases, *Cell 59*, 219−228.
31. Morrison, A., Bell, J. B., Kunkel, T. A., and Sugino, A. (1991) Eukaryotic DNA polymerase amino acid sequence required for 3′−5′ exonuclease activity, *Proc. Natl. Acad. Sci. U.S.A. 88*, 9473−9477.
32. Blanco, L., Bernad, A., and Salas, M. (1992) Evidence favouring the hypothesis of a conserved 3′−5′ exonuclease active site in DNA-dependent DNA polymerases, *Gene 112*, 139−144.
33. de Vega, M., Lazaro, J. M., Salas, M., and Blanco, L. (1998) Mutational analysis of phi29 DNA polymerase residues acting as ssDNA ligands for 3′−5′ exonucleolysis, *J. Mol. Biol. 279*, 807−822.
34. Blanco, L., Bernad, A., Blasco, M. A., and Salas, M. (1991) A general structure for DNA-dependent DNA polymerases, *Gene 100*, 27−38.
35. Wang, J., Yu, P., Lin, T. C., Konigsberg, W. H., and Steitz, T. A. (1996) Crystal structures of an NH_2-terminal fragment of T4 DNA polymerase and its complexes with single-stranded DNA and with divalent metal ions, *Biochemistry 35*, 8110−8119.
36. Curley, J. F., Joyce, C. M., and Piccirilli, J. A. (1997) Functional Evidence that the 3′−5′ Exonuclease Domain of *Escherichia coli* DNA Polymerase I Employs a Divalent Metal Ion in Leaving Group Stabilization, *J. Am. Chem. Soc. 119*, 12691−12692.
37. Derbyshire, V., Pinsonneault, J. K., and Joyce, C. M. (1995) Structure−function analysis of 3′ → 5′-exonuclease of DNA polymerases, *Methods Enzymol. 262*, 363−385.
38. Sandbrook, J., Fritsch, E. F., and Maniatis, T. (1980) *Molecular Cloning: A Laboratory Manual*, 2nd ed., Cold Spring Harbor Laboratory Press, Plainview, NY.
39. Grasby, J. A., and Connolly, B. A. (1992) Stereochemical outcome of the hydrolysis reaction catalyzed by the EcoRV restriction endonuclease, *Biochemistry 31*, 7855−7861.
40. Ellis, K. J., and Morrison, J. F. (1982) Buffers of constant ionic strength for studying pH-dependent processes, *Methods Enzymol. 87*, 405−426.

41. Elisseeva, E., Mandal, S. S., and Reha-Krantz, L. J. (1999) Mutational and pH studies of the 3′ → 5′ exonuclease activity of bacteriophage T4 DNA polymerase, *J. Biol. Chem. 274*, 25151−25158.
42. Cowart, M., Gibson, K. J., Allen, D. J., and Benkovic, S. J. (1989) DNA substrate structural requirements for the exonuclease and polymerase activities of procaryotic and phage DNA polymerases, *Biochemistry 28*, 1975−1983.
43. de Vega, M., Ilyina, T., Lazaro, J. M., Salas, M., and Blanco, L. (1997) An invariant lysine residue is involved in catalysis at the 3′−5′ exonuclease active site of eukaryotic-type DNA polymerases, *J. Mol. Biol. 270*, 65−78.
44. Braithwaite, D. K., and Ito, J. (1993) Compilation, alignment, and phylogenetic relationships of DNA polymerases, *Nucleic Acids Res. 21*, 787−802.
45. Derbyshire, V., Freemont, P. S., Sanderson, M. R., Beese, L., Friedman, J. M., Joyce, C. M., and Steitz, T. A. (1988) Genetic and crystallographic studies of the 3′,5′-exonucleolytic site of DNA polymerase I, *Science 240*, 199−201.
46. Brautigam, C. A., and Steitz, T. A. (1998) Structural principles for the inhibition of the 3′−5′ exonuclease activity of *Escherichia coli* DNA polymerase I by phosphorothioates, *J. Mol. Biol. 277*, 363−377.
47. Frey, M. W., Nossal, N. G., Capson, T. L., and Benkovic, S. J. (1993) Construction and characterization of a bacteriophage T4 DNA polymerase deficient in 3′ → 5′ exonuclease activity, *Proc. Natl. Acad. Sci. U.S.A. 90*, 2579−2583.
48. Gupta, A. P., Benkovic, P. A., and Benkovic, S. J. (1984) The effect of the 3′,5′ thiophosphoryl linkage on the exonuclease activities of T4 polymerase and the Klenow fragment, *Nucleic Acids Res. 12*, 5897−5911.
49. Spitzer, S., and Eckstein, F. (1988) Inhibition of deoxyribonucleases by phosphorothioate groups in oligodeoxyribonucleotides, *Nucleic Acids Res. 16*, 11691−11704.
50. Lam, W. C., Thompson, E. H., Potapova, O., Sun, X. C., Joyce, C. M., and Millar, D. P. (2002) 3′−5′ exonuclease of Klenow fragment: role of amino acid residues within the single-stranded DNA binding region in exonucleolysis and duplex DNA melting, *Biochemistry 41*, 3943−3951.
51. Herschlag, D., Piccirilli, J. A., and Cech, T. R. (1991) Ribozyme-catalyzed and nonenzymatic reactions of phosphate diesters: rate effects upon substitution of sulfur for a nonbridging phosphoryl oxygen atom, *Biochemistry 30*, 4844−4854.
52. Polesky, A. H., Dahlberg, M. E., Benkovic, S. J., Grindley, N. D., and Joyce, C. M. (1992) Side chains involved in catalysis of the polymerase reaction of DNA polymerase I from *Escherichia coli*, *J. Biol. Chem. 267*, 8417−8428.

BI0302292